First Observation of the Earth's Permanent Free Oscillations on Ocean Bottom Seismometers

M. Deen, E. Wielandt, E. Stutzmann, W. Crawford, G. Barruol, K. Sigloch

AGU PUBLICATIONS

Geophysical Research Letters

RESEARCH LETTER
10.1002/2017GL074892

Key Points:
- Earth's eigenmodes observed at ocean bottom in the absence of earthquakes
- Linear regression and frequency transfer functions are effective methods to remove tilt and compliance
- Autocorrelation of continuous data and windowing to show eigenmodes at PREM frequencies

Supporting Information:
- Supporting Information S1

Correspondence to:
M. Deen,
deen@ipgp.fr

Citation:
Deen, M., Wielandt, E., Stutzmann, E., Crawford, W., Barruol, G., & Sigloch, K. (2017). First observation of the Earth's permanent free oscillations on ocean bottom seismometers. *Geophysical Research Letters*, *44*. https://doi.org/10.1002/2017GL074892

Received 10 JUL 2017
Accepted 25 SEP 2017
Accepted article online 6 OCT 2017

First Observation of the Earth's Permanent Free Oscillations on Ocean Bottom Seismometers

M. Deen[1], E. Wielandt[2], E. Stutzmann[1], W. Crawford[1], G. Barruol[1,3], and K. Sigloch[4]

[1]Institut de Physique du Globe de Paris, Sorbonne Paris Cite, Paris, France, [2]Institute of Geophysics, University of Stuttgart, Stuttgart, Germany, [3]Laboratoire GéoSciences Réunion, Université de La Réunion, Institut de Physique du Globe de Paris, Sorbonne Paris Cité, UMR7154 CNRS, Université Paris Diderot, Saint Denis, France, [4]Department of Earth Sciences, University of Oxford, Oxford, UK

Abstract The Earth's hum is the permanent free oscillations of the Earth recorded in the absence of earthquakes, at periods above 30 s. We present the first observations of its fundamental spheroidal eigenmodes on broadband ocean bottom seismometers (OBSs) in the Indian Ocean. At the ocean bottom, the effects of ocean infragravity waves (compliance) and seafloor currents (tilt) overshadow the hum. In our experiment, data are also affected by electronic glitches. We remove these signals from the seismic trace by subtracting average glitch signals; performing a linear regression; and using frequency-dependent response functions between pressure, horizontal, and vertical seismic components. This reduces the long period noise on the OBS to the level of a good land station. Finally, by windowing the autocorrelation to include only the direct arrival, the first and second orbits around the Earth, and by calculating its Fourier transform, we clearly observe the eigenmodes at the ocean bottom.

1. Introduction

The Earth's hum is the continuous free oscillations of the Earth recorded at long period in the absence of earthquakes (Nishida et al., 2000). The hum was first observed on a superconducting gravimeter in Antarctica (Nawa et al., 1998), followed by observations on a STS-1Z seismometer (Kobayashi & Nishida, 1998; Tanimoto et al., 1998) and on a STS-2 seismometer (Widmer-Schnidrig, 2003). These studies all excluded oscillations created by large earthquakes ($M_w > 5.5$). Several generating mechanisms have been proposed to explain the hum signal. Cumulative excitation by small earthquakes was shown to be ineffective as a generation mechanism (Kobayashi & Nishida, 1998; Suda et al., 1998; Tanimoto & Um, 1999). The hum was also proposed to be induced by acoustic resonance between the atmosphere and the solid Earth, but this can only explain part of its amplitude (Lognonne et al., 1998; Watada & Kanamori, 2010). Later, different generation mechanisms proposed that what they have in common is that the hum is generated by ocean infragravity waves (Ardhuin et al., 2015; Bromirski, 2009; Nishida, 2013; Rhie & Romanowicz, 2004, 2006; Tanimoto, 2005; Traer & Gerstoft, 2014; Webb, 2007).

Since its discovery, the hum has been observed at a large number of terrestrial stations. Free oscillations induced by a large earthquake (M = 8.1) were observed on a few ocean bottom seismometers (OBSs) deployed in the Lesser Antilles region (Bécel et al., 2011), but no one has observed the Earth's hum at an OBS during periods of seismic quiescence. A low noise level is needed to observe the small signal amplitude of the hum. At the ocean bottom, the noise level at long periods is generally much higher than at land stations, due to several factors such as ocean wave loading (compliance) and seafloor currents (tilt) (Crawford & Webb, 2000; Webb & Crawford, 1999). Burying the OBS in sediment or in a borehole can remove part of this noise (Montagner et al., 1994; Romanowicz et al., 1998; Collins et al., 2001; Stephen et al., 2003; Sutherland et al., 2004; Crawford et al., 2006) but is technically challenging and requires the appropriate tools, expertise, and funding. In the case of free-fall OBS (as in this study), noise reduction can only be performed by processing the data after the period of deployment.

The objective of this research is to lower the noise level on vertical broadband OBS data and to identify the permanent normal modes of the Earth during periods of seismic quiescence. Although several authors were able to reduce low-frequency noise (Crawford & Webb, 2000; Dahm et al., 2006; Dolenc et al., 2007; Stutzmann et al., 2001; Taira et al., 2014), the hum remains challenging to observe. With our proposed noise reduction methods, we improve the data quality of broadband OBS so that the data become useful for a

variety of applications. For example, the Earth's hum can be used to study the Earth's deep interior (Nishida et al., 2009, Haned et al., 2015). Station coverage in the oceans is much sparser than on land, leaving great parts of the Earth uncovered. Including OBS data can substantially increase station coverage and hence improve tomography models to help understand the Earth's deep interior.

For the removal of tilt and compliance noise from the vertical channel of the seismometer we use two methods: a linear regression (Zürn & Widmer, 1995) and frequency-dependent response functions (Crawford & Webb, 2000). Compliance is the vertical deformation of the seafloor under pressure forcing from ocean infragravity waves. It can be quantified by correlating measurements of pressure and of vertical seismic displacement. Tilt results from the drag of seafloor currents on the OBS or on seafloor topography. Even a slight inclination of the sensor can cause tilt noise to be projected from the horizontal components onto the vertical component (Crawford & Webb, 2000).

Besides the physical tilt and compliance noises, our data unfortunately also contain nearly periodic, impulsive electronic glitches that increase the noise level. The glitches are present in all broadband OBS stations of our data set. The origin of the largest glitch is a transient communication signal enhanced by the wiring of the instrument. A more detailed explanation and suggestion for instrument improvement can be found in Text S1 in the supporting information. In this article, we develop a time domain a posteriori method to remove such glitches using an average glitch waveform that is matched to each individual glitch in time and amplitude.

We first present the RHUM-RUM (Réunion Hotspot and Upper Mantle-Réunions Unterer Mantel) data set (Barruol & Sigloch, 2013) we used and the problems we encountered with electronic glitches in the broadband seismograms. Next, we introduce a method for removing such glitches. We then describe the processing of data for tilt and compliance removal. Finally, we use a windowed autocorrelation of the time series to enhance the hum signal in the Fourier transform. This allows us to observe the hum at the ocean bottom and to compare it to a reference, high-quality GEOSCOPE land station TAM in Tamanrasset Algeria.

2. The RHUM-RUM Data Set

In the RHUM-RUM experiment, a total of 57 free-fall OBS stations were deployed in the Indian Ocean around La Réunion Island, east of Madagascar, over an area of 2,000 km × 2,000 km from September 2012 to November 2013 (Barruol et al., 2012; Barruol & Sigloch, 2013). The instruments of the RHUM-RUM project include 48 wideband DEPAS OBS and 9 broadband OBS that were manufactured at the Scripps Institution of Oceanography and at the INSU-IPGP OBS facility. The broadband OBS are equipped with a Nanometrics Trillium broadband seismometer with a corner period of 240 s and a long period differential pressure gauge (Cox et al., 1984). Seven of the 9 broadband stations had complete seismometer and pressure data. Stähler et al. (2016) provide a comprehensive report on data quality. Here we use two of the nine broadband OBSs from the RHUM-RUM project: RR28, the station with the best data quality and the longest time of recording, together with station RR34. Stations RR28 and RR34 were dropped freely at (−22.7152 latitude, 53.1594 longitude) and (−32.0783 latitude, 52.2114 longitude), respectively, to a depth of 4,540 m and 4,260 m, respectively, and on 150 m versus 410 m thick sediments (Whittaker et al., 2013).

3. Processing Ocean Bottom Data I: Earthquake and Glitch Removal

We resample the data to 0.625 mHz and filter between 3 and 30 mHz—more information in supporting information S1—to visualize the glitch. Figure 1b shows the result for the vertical channel as a red trace, in which we can easily discern the glitch signal, which recurs every 3,620.3 s for station RR28.

From the continuous time series, we null time periods corresponding to earthquakes of magnitudes above 6 for a duration of 1.5 days per 1 M_w increase above the threshold of $M_w = 5.85$. That is, for 5.4 h at magnitude 6, for 41.4 h at magnitude 7, for example. To remove occasional other high-amplitude signals, we clip the vertical channel data above the glitch amplitude (−5,000 and +5,000 for station RR28).

From the preprocessed, earthquake-free vertical trace, we can now remove the glitches in several steps: first, we determine the average periodicity of the glitches, which can vary from station to station. We ensure that the period is stable by cutting the trace in data pieces whose length is the glitch period and aligning these data pieces. Figure 1b shows the alignment for station RR28 with the colored negative and positive values

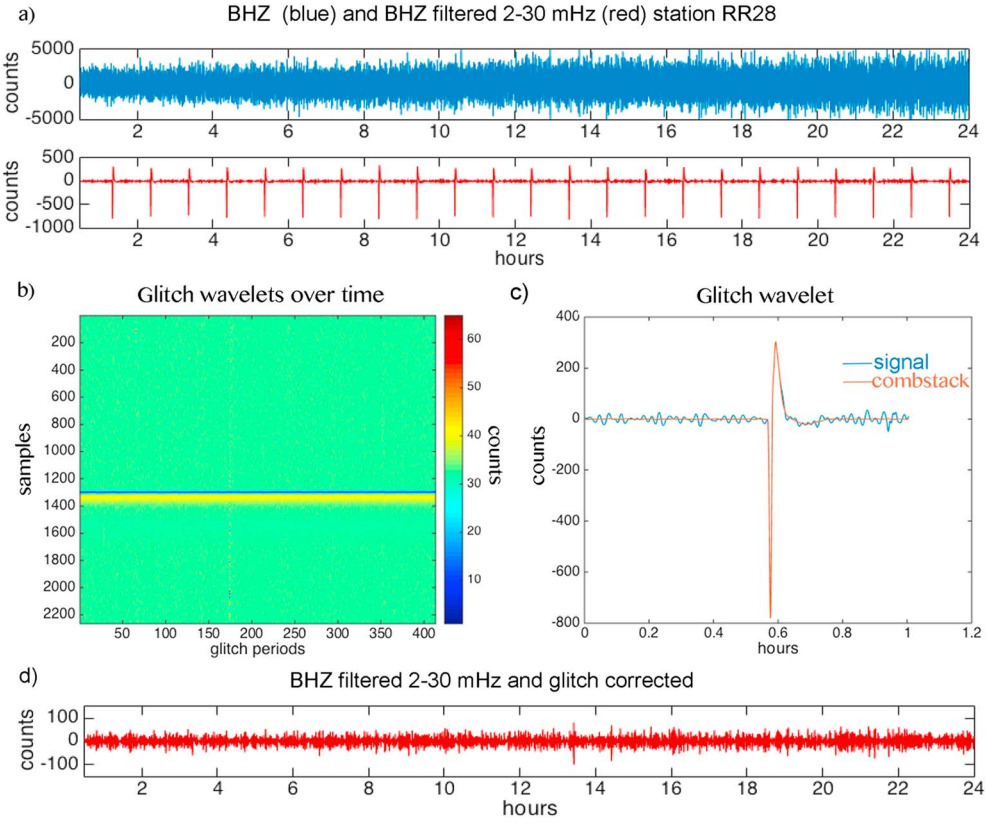

Figure 1. Glitch removal example at station RR28. (a) The blue curve represents a raw trace of the first day of December 2012 with amplitudes between −5,000 and 5,000 counts. In red the same trace is filtered between 2 and 30 mHz, so that the primary and secondary microseismic signals are removed, reducing the noise level so that the glitch of period 3,620.3 s and amplitude between −1,000 and 500 becomes visible. (b) The horizontal aligning of the tranches of a month length trace with the glitch period assures the correct glitch period and its continuity over the chosen time window. (c) The first glitch is shown in blue and the comb stack—the cross correlation between the comb and the trace of a month's length—in red. (d) We show the same day length trace as Figures 1a and 1b after correcting for the glitch wavelet.

lining up for all hourly glitches. At other times, we occasionally see jumps in the glitch period, forcing us to subdivide the monthly data set. We adjust the periodicity so that the blue and yellow lines align horizontally.

Second, we stack the aligned data pieces by correlating the signal with a comb. The comb was constructed in the frequency domain in order to allow for a glitch periodicity that is not an integer multiple of the sampling interval. In Figure 1c the first glitch wavelet is shown in blue and the average glitch (normalized stacked pulse) in red. The comb is then convolved with the normalized stacked pulse to produce a series of average glitches. This trace is used to mark the position of the glitches in the time series and is later used to suppress residuals from the steepest part of the pulse.

For glitch removal, we now fit a sum of one left-shifted and one right-shifted average pulse to each glitch in the data. This is a fit with two free parameters, roughly equivalent to fitting the amplitude and the position within plus or minus one sampling interval. The resulting trace is shown in Figure 1d. Figure 2 shows the noise reduction by glitch removal (from orange to black) for the month December 2012 for station RR28.

4. Processing Ocean Bottom Data II: Tilt and Compliance Removal

In order to reduce noise from the ocean environment—tilt and compliance—we use two methods: one based on linear regression (Zürn & Widmer, 1995) that we adapted for OBS data, and one based on frequency response functions (Crawford & Webb, 2000). The linear regression is based on the overall correlation of the vertical trace with an estimation of the double derivative of the pressure, the horizontal channels and an estimation of the gradient of the pressure (explained in supporting information S1). The frequency response functions are based on the coherence between the four channels within a station.

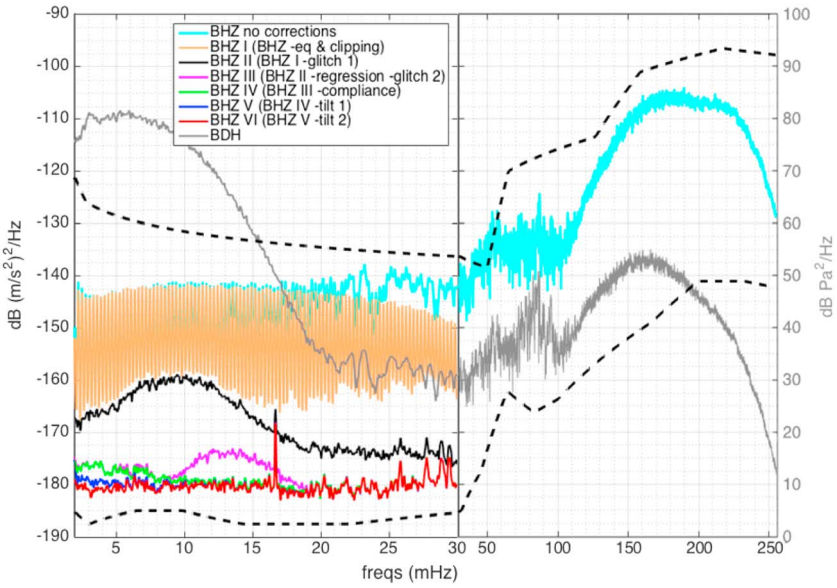

Figure 2. Processing steps shown for average spectra—window length of 4 h—of December 2012 for station RR28. The cyan curve shows the raw data for the vertical component BHZ between 2 and 250 mHz. The orange curve shows the effect of clipping and earthquake removal ($M_w > 5.85$). It is filtered between 2 and 30 mHz and shows the oscillations of the first glitch. To go from the orange to the black curve we remove the hourly glitches. From black to magenta we perform clipping and a linear regression and remove the remaining glitches (consult text for detailed explanation). Next, we use a frequency response function between the pressure channel (in gray) and the vertical component (magenta) to remove the effect of compliance, resulting in the green curve. The blue and red curves show the removal of the tilt-related coherence between channel BHZ and channel BH2 and BH1, respectively. The black dashed lines indicate the low and high noise model of Peterson (1993). The red curve is down to −182 dB in acceleration, comparable to a good land station. A peak at 60 s period remains in the red curve but, due to its high frequency, poses no problems for the scope of this research.

Both methods make use of other channels that are more sensitive to this noise than the vertical channel. The pressure channel is more sensitive to recording pressure fluctuation of infragravity ocean waves above the OBS than the vertical seismic channel (Crawford et al., 2006). The horizontal seismic channels are more sensitive to currents moving around the OBS than the vertical seismic channel (Crawford et al., 2006).

In the linear regression method, we assume that a certain percentage of the pressure and horizontal channels is recorded on the vertical channel. We solve a system of linear equations to find frequency-independent factors that describe this percentage. The factors describe the relation between the vertical channel and (1) an estimation of the double derivative of the pressure, (2) the horizontal channels, and (3) an estimation of the gradient of the pressure, chosen partly empirically. Supporting information S1 contains a detailed description on the choice of these empirical factors. The factors are not exactly frequency independent, but this approximation provides significant noise reduction: for station RR28, the raw signal rms is reduced from 11.36 counts before regression to 3.49 counts after regression (about 1/3 of the previous rms amplitude). At this low noise level, a second glitch type becomes visible with a period of 2.6 h, which we remove using the same method as described before. This further reduces the noise level to a signal rms of 2.53 counts (about 1/5 of the original rms amplitude) for the example of the month December 2012 of station RR28. At this stage we detect another, very small glitch with a period of 24 h, for which we again apply the above glitch removal method. In Figure 2 the effect of linear regression and these longer period glitch removals is visible between the black and magenta curve.

Even after the linear regression, the residual trace can still contain some tilt and compliance noise for certain frequencies. In Figure 2 we clearly see a remaining compliance effect between 10 and 17 mHz (in magenta), whose shape resembles the increase in spectral amplitude of the pressure channel (in gray). The linear regression is not frequency-dependent, and to ensure that we remove noise for all frequencies, we also use an alternative frequency-dependent method that is readily available (Crawford & Webb, 2000). The linear regression and the frequency dependent method give similar but not identical results for frequencies below 5 mHz. A combination of both methods makes it possible to treat the data up to 30 mHz. Therefore, after linear regression, we follow the method of Crawford and Webb (2000), who uses a frequency-dependent response

function to remove tilt and compliance noise. The main signal on the pressure channel is from the pressure forcing responsible for compliance. The vertical channel records compliance among other signals. This way, the frequency response function describes the vertical acceleration of the seismometer that is due to the pressure forcing recorded on the pressure channel.

$$\boldsymbol{R_{zp}}(\boldsymbol{f}) = \gamma_{\boldsymbol{zp}}(\boldsymbol{f})\sqrt{\frac{\boldsymbol{G_{zz}}(\boldsymbol{f})}{\boldsymbol{G_{pp}}(\boldsymbol{f})}} \tag{1}$$

In which $\boldsymbol{G_{zz}}(\boldsymbol{f})$ and $\boldsymbol{G_{pp}}(\boldsymbol{f})$ are the power spectral densities of the vertical seismometer channel Z and pressure channel P, respectively, and $\gamma_{\boldsymbol{zp}}(\boldsymbol{f})$ complex coherency between the two channels.

We use the frequency response function, $\boldsymbol{R_{zp}}(\boldsymbol{f})$, to remove the compliance effect, $\boldsymbol{R^*_{zp}}(\boldsymbol{f})\boldsymbol{P}(\boldsymbol{f})$ (where the asterisk indicates the complex conjugate), from the vertical channel $Z(f)$.

$$\boldsymbol{Z}'(\boldsymbol{f}) = \boldsymbol{Z}(\boldsymbol{f}) - \boldsymbol{R^*_{zp}}(\boldsymbol{f})\boldsymbol{P}(\boldsymbol{f}) \tag{2}$$

The green curve $Z'(f)$ in Figure 2 shows the effect of compliance removal on the vertical channel. Next, we remove all tilt noise from the cleaned vertical, using the same routine for different channels. We replace the pressure channel $P(f)$ by the horizontal compliance-corrected channel $H_1'(f)$ and $R^*_{zp}(f)$ by $R^*_{zh_1'}(f)$. Here we assume that the horizontal channels record predominantly tilt signal and the vertical channel records tilt among other signals. This results in $Z''(f)$, whose average is represented as the blue curve in Figure 2. After repeating the procedure with the other horizontal channel, we arrive at the cleaned vertical channel $Z''(f)$ (red curve in Figure 2). The noise level is as low as -182 dB acceleration, which corresponds to a good land station and is close to the low noise level of Peterson (1993).

5. Method for Finding the Hum at the OBS

With the OBS long-period noise level reduced to that of a good land station, the challenge remains to observe the Earth's fundamental spheroidal modes in the absence of earthquakes. Most observations have been done by calculating the power spectral density of the continuous quiet data (Kobayashi & Nishida, 1998; Nishida and Kobayashi, 1999; Nawa et al., 2000; Kurrle & Widmer-Schnidrig, 2008). This can require a large volume of earthquake-free data to stack so that the signal-to-noise level is high enough for the small hum signal to be observed at the ocean bottom. Here we introduce a method that increases the signal-to-noise level without requiring very long time series.

We start by calculating the autocorrelation over a period of 2 days in which earthquakes are removed. We use 50% overlapping windows of 2 days length. We assume that the hum consists predominantly of surface waves and that generating fundamental spheroidal modes requires constructive interference of multiple orbits around the Earth. The benefit of using the autocorrelation is that we can identify the multiple orbits by their predictable lag time. We calculate the autocorrelation up to a maximum lag time of 11 h, which includes the first and second orbits around the Earth. In order to improve the signal-to-noise ratio, we then null everything that is not in a window around the zero lag or the first and second circuits (for both positive and negative lag times). Supporting information S2 provides a more detailed explanation of the autocorrelation and the effect of this nulling.

Finally, we calculate the Fourier transform of the windowed autocorrelation, normalized by the length of the autocorrelated series. In some of the autocorrelation windows, part of the signal, or even all of it, may be zero as a consequence of the nulling of data during the time window of a strong earthquake. Since we are interested in only the hum signal, we calculate and subtract the nonhum base noise level from the PSD. In supporting information S2 and Figure S2 in the supporting information we present a detailed explanation on this background-noise removal. With the background noise removed, we can make a comparison between stations. We apply the method to two OBS (RR28 and RR34) and one high-quality GEOSCOPE land station, TAM in Algeria, which is chosen as a low-noise terrestrial reference station (Stutzmann et al., 2000) and is unaffected by electronic glitch noise. We now investigate and compare the hum on those three stations for the year 2013.

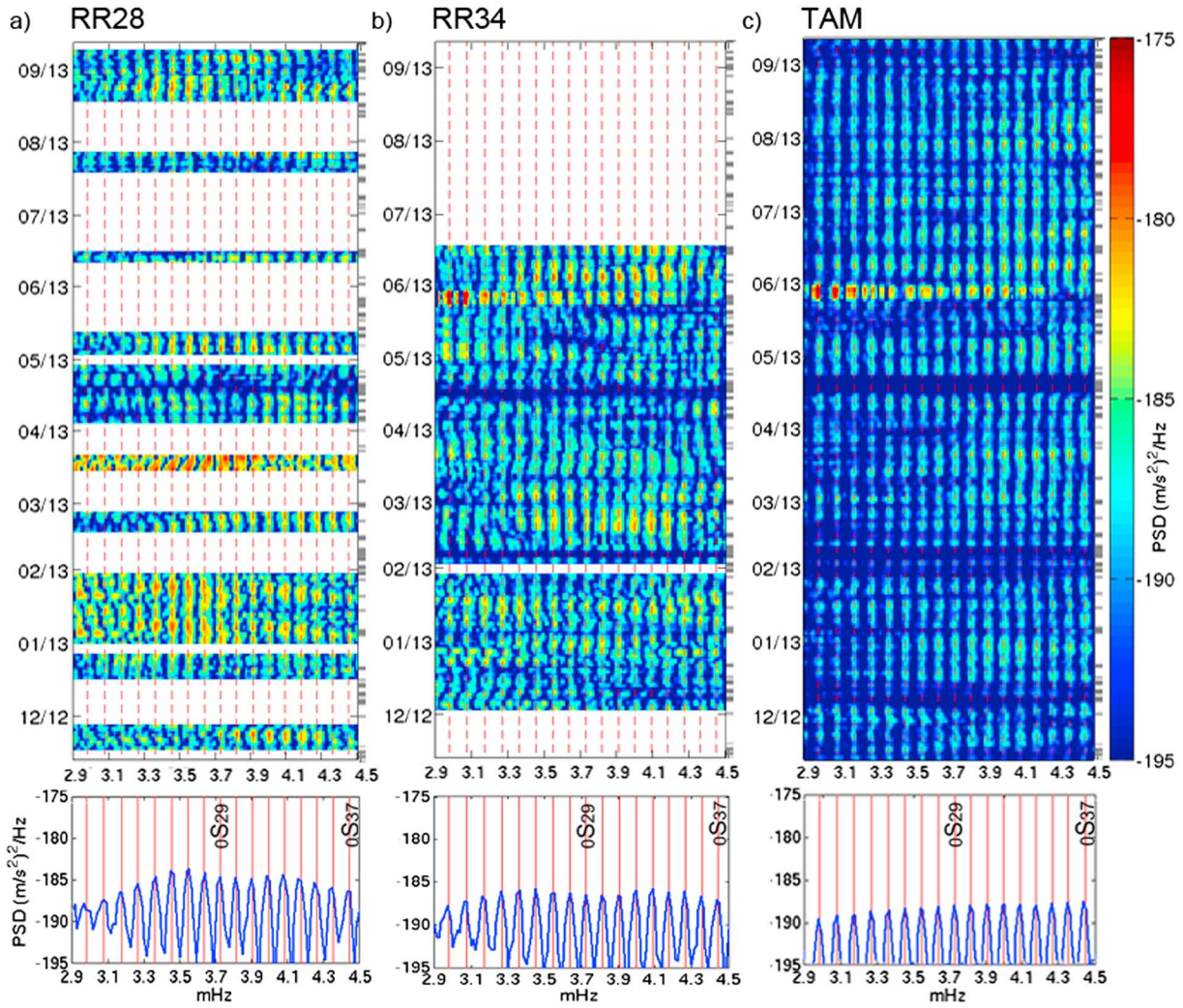

Figure 3. Temporal continuity of the eigenmodes presented for stations (a) RR28, (b) RR34, and (c) TAM. Fourier transform taken on autocorrelation windows of 50% overlap. The light to red colors indicate an elevated spectral amplitude of autocorrelation, equal to power spectral density (PSD). The vertical dashed red lines are the eigenfrequencies of the PREM model. The gray blocks indicate missing data due to earthquake removal. The horizontal white patches represent the absence of data the PREM eigenfrequencies overlap on the spectral modes from the data for all stations. The spectral modes are continuous in time for all stations. (bottom) Mean of the PSD shown above. The eigenmodes from the data of three stations are plotted in blue and coincide with the theoretical eigenfrequencies of the PREM Earth model in red. All stations show clear peaks at the PREM eigenfrequencies. The amplitudes of the eigenmodes, corrected for the instrument self-noise, show little variation between the stations (within an order of magnitude), nor between the different eigenfrequencies.

6. The Hum Observed at Two OBSs and on Land

Figure 3 shows the results of the Fourier transform of the windowed autocorrelations as a function of time (top images) and the median of all data between December 2012 and October 2013 for the stations RR28, RR34, and TAM (bottom images), all corrected for station self-noise. The bottom images clearly evidence the eigenmodes observed at the ocean and terrestrial stations, with peaks at the eigenfrequencies of the fundamental spheroidal modes of the preliminary reference Earth model (PREM) (Dziewonski & Anderson, 1981) between 2.9 and 4.5 mHz. The observed hum amplitudes are of the same order of magnitude on all three stations: the median amplitude of the modes varies less than 5 dB across stations. For all stations, the amplitude is lower than −185 dB in acceleration for most frequencies between 2.9 and 4.5 mHz. At most frequencies between 2.9 and 4.5 mHz, the OBS stations show slightly higher median amplitude than TAM. Note that this amplitude is lower than the low noise model of Peterson (1993) because we subtracted the nonhum background noise. The observed amplitude should therefore correspond to the hum amplitude and demonstrate how small this signal really is. For the absolute noise level we refer to Figure S2.

Another point of interest is the modes at which acoustic coupling between atmosphere and solid Earth takes place: 3.704 mHz for 0S29 and at 4.348 mHz for 0S37 (Nishida et al., 2000). In our data, we see no significant difference between the amplitudes of these modes compared to other modes on any of the stations, nor do we observe a significant difference in average amplitude between these modes recorded at OBS versus land stations. In addition, we compared the seasonal variation by taking the average of the uncoupled modes and comparing it to 0S29 and 0S37 in a similar way as Nishida (2013), for RR28, RR34, and TAM separately. Nishida (2013) found the seasonal variation of mode 0S29 to be 40% higher than that of the noncoupled modes, whereas we did not. In summary, we do not observe acoustic mode coupling on our OBS stations or on land station TAM.

The top panels of Figure 3 show the temporal continuity of the eigenmodes by plotting the power spectra for windows of 2 days with 50% overlap. The white spaces of stations RR28 and RR34 correspond to (long) periods of missing data or data that were not used because we were not able to remove the glitches in the noisiest parts of the data. The time intervals of removed earthquakes are shown in gray on the right side for each station. At these times, we occasionally observe an absence of light colored vertical lines due to the nulling of data for earthquake removal. All three stations (RR28 in Figure 3a, RR34 in Figure 3b, and TAM in Figure 3c) show clear light colored vertical lines that correspond to the PREM eigenfrequencies (plotted as dashed red lines).

The amplitudes are not constant over time, but we do not observe any significant seasonal variation of the hum at frequencies between 2.9 and 4.5 mHz. Tanimoto and Um (1999), Ekström (2001), and Nishida and Fukao (2007) did report seasonal variations. These studies were done in a wider frequency band (between 2 and 7 mHz). Rhie and Romanowicz (2006) saw no seasonal variation around a frequency of 4.1 mHz. We note that the OBS stations are located in the Indian Ocean, open to southern hemisphere winter storms, but experiencing cyclones during northern hemisphere summer, and station TAM is in the African continent not far from the equator. Their particular positions could therefore explain the absence of detectable hum seasonal variations. In March 2013 at station RR28 we observe some shifted, widened high-amplitude blobs, which we attribute to an elevated noise level that rendered the glitch removal less effective. In May 2013 we observe increased amplitude of the normal modes for frequencies below 4 mHz at stations RR34 and TAM. Elevated amplitudes occur only during a few days and therefore do not appear to be related to any seasonal variation. Prior on 24 May was a large earthquake in the Sea of Okhotsk of magnitude M_w 8.3. From 10 to 17 May 2013 the tropical cyclone Mahasen moved over the northern Indian Ocean, and the eruption of Pavlov Volcano in the Aleutian Arc took place from 13 to 18 May 2013. Previous studies had observed acoustic coupling during a volcanic eruption (e.g., Kanamori & Mori, 1992; Widmer & Zürn, 1992) as an increase in amplitudes of modes 0S29 and 0S37. We do not observe such an increase in mode amplitudes for these specific modes in the period of the Pavlov Volcano eruption.

7. Conclusions

We demonstrate the presence of eigenmodes at two ocean bottom seismometers for the first time. We do so by noise reduction and calculation of the autocorrelation of the seismograms. We successfully removed electronic glitches of varying periodicity from vertical OBS data, which reduced the noise level by 28 dB. Our technique filters the data and subtracts an average glitch wavelet, adjusted in position and amplitude. We use linear regression with an estimation of the double derivative of the pressure, the horizontal channels and an estimation of the gradient of the pressure as inputs to reduce the seismic noise level on the vertical seismometer channel and remove the long period glitches. By further removing compliance and tilt using frequency response functions based on the coherence between different seismometer and pressure channels, we were able to reduce the noise level by another 8 dB. The final noise level at the OBS is only around −182 dB in acceleration, which is close to the noise level of a quiet land station (Peterson, 1993).

On the denoised time series, we observe the hum signal on the ocean bottom, by windowing the autocorrelation around the direct arrival and the first and second orbits around the Earth, followed by a Fourier transform. We observe very clear peaks that coincide with the Earth's theoretical eigenfrequencies between 2.9 and 4.5 mHz. The same procedure applied to reference land station TAM in southern Algeria shows a hum signal of similar amplitude on land and on the ocean bottom. We demonstrate the continuous presence of

these modes over the whole 11 monthlong period of deployment of the OBS but observe no clear seasonal variation of the hum between 2.9 and 4.5 mHz.

Acknowledgments
We would like to thank the RHUM-RUM project (www.rhum-rum.net), funded by ANR (Agence Nationale de la Recherche) in France (project ANR-11-BS56-0013) and by DFG (Deutsche Forschungsgemeinschaft) in Germany (grants SI1538/2-1 and SI1538/4-1). Additional support was provided by CNRS (Centre National de la Recherche Scientifique, France). We also thank INSU-IPGP (Institut National des Sciences de l'Univers-Institut de Physique du Globe de Paris, France) for providing the broadband ocean-bottom seismometers. The RHUM-RUM data set (http://dx.doi.org/10.15778/RESIF.YV2011) is hosted and served by the French RESIF data center (http://seismology.resif.fr) under the FDSN network code YV. Data are available from the authors on request before they become freely available by the end of 2017. Thanks to all cruise participants on R/V *Marion Dufresne*, cruise MD192 and on R/V *Meteor*, cruise M101. This article is based upon work from COST Action ES1401-TIDES, supported by COST (European Cooperation in Science and Technology) by constructive discussions during the workshops in Bologna 2015 and in Sesimbra 2016. We would like to thank Ruedi Widmer and Walter Zürn at the Black Forest Observatory for hosting us and sharing their knowledge on data processing. Finally, we would like to thank Jean-Marie Saurel from IPGP for technical input on the glitch explanation. This work is funded by ANR MIMOSA (ANR-14-CE01-0012). This is IPGP contribution number 3892.

References

Ardhuin, F., Gualtieri, L., & Stutzmann, E. (2015). How ocean waves rock the Earth: Two mechanisms explain microseisms with periods 3 to 300 s. *Geophysical Research Letters*, *42*, 765–772. https://doi.org/10.1002/2014GL062782

Barruol, G., & Sigloch, K. (2013). Investigating la Réunion hot spot from crust to core. *Eos, Transactions American Geophysical Union*, *94*(23), 205–207. https://doi.org/10.1002/2013EO230002

Barruol, G., Sigloch, K., & the RHUM-RUM group (2012). RHUM-RUM experiment, 2011–2015, code YV (réunion hotspot and upper mantle réunion's unterer mantel) funded by ANR, DFG, CNRS-INSU, IPEV, TAAF, instrumented by DEPAS, INSU-OBS, AWI and the universities of muenster, bonn, la réunion, RESIF - . Reseau Sismologique et géodésique Français. https://doi.org/10.15778/RESIF.YV2011

Bécel, M., Laigle, A., Diaz, J., Montagner, J.-P., & Him, A. (2011). Earth's free oscillations recorded by free-fall obs ocean-bottom seismometers at the lesser Antilles subduction zone. *Geophysical Research Letters*, *38*, L24305. https://doi.org/10.1029/2011GL049533

Bromirski, P. D. (2009). Earth vibrations. *Science*, *324*(5930), 1026–1027. https://doi.org/10.1126/science.117183

Cox, C., Deaton, T., & Webb, S. (1984). A deep-sea differential pressure gauge. *Journal of Atmospheric and Oceanic Technology*, *1*, 237–246. https://doi.org/10.1175/1520%E2%80%930426(1984)001%3C237:ADSDPG%3E2.0.CO;2

Collins, J., Vernon, F., Orcutt, J., Stephen, R., Peal, K., Wooding, F., Spiess, F., & Hildebrand, J. (2001). Broadband seismology in the oceans: Lessons from the oceans seismic network pilot experiment. *Geophysical Research Letters*, *28*(1), 49–52. http://doi.org/10.1029/2000GL011638

Crawford, W., Stephen, R., & Bolmer, S. T. (2006). A second look at low-frequency marine vertical seismometer data quality at the OSN-1 site off Hawaii for seafloor, buried and borehole emplacements. *Bulletin of the Seismological Society of America*, *96*(5), 1952–1960. https://doi.org/10.1785/0120050234

Crawford, W., & Webb, S. (2000). Identifying and removing tilt noise from low-frequency (<0.1 Hz) seafloor vertical seismic data. *Bulletin of the Seismological Society of America*, *90*(4), 952–963.

Dahm, T., Tilmann, F., & Morgan, J. P. (2006). Seismic broadband ocean bottom data and noise observed with free-fall stations: Experiences from long-term deployments in the North Atlantic and Tyrrhenian Sea. *Bulletin of the Seismological Society of America*, *96*(2), 647–664. https://doi.org/10.1785/0120040064

Dolenc, D., Romanowicz, B., & Uhrhammer, R. (2007). Identifying and removing noise from the Monterey ocean bottom broadband seismic station (MOBB) data. *Geochemistry, Geophysics, Geosystems*, *8*, Q02005. https://doi.org/10.1029/2006GC001403

Dziewonski, A. M., & Anderson, D. L. (1981). Preliminary reference Earth model. *Physics of the Earth and Planetary Interiors*, *25*(4), 297–356. https://doi.org/10.1016/0031-9201(81)90046-7

Ekström, G. (2001). Time domain analysis of Earth's long-period background seismic radiation. *Journal of Geophysical Research*, *106*, 26,483–26,493. https://doi.org/10.1029/2000JB000086

Haned, A., Stutzmann, E., Schimmel, M., Diselev, S., Davaille, A., & Yelles-Chaouche, A. (2015). Global tomography using seismic hum. *Geophysical Journal International*, *204*(2), 1222–1236. https://doi.org/10.1093/gji/ggv516

Kanamori, H., & Mori, J. (1992). Harmonic excitation of mantle Rayleigh waves by the 1991 eruption of mount Pinatubo, Philippines. *Geophysical Research Letters*, *19*, 721–724. https://doi.org/10.1029/92GL00258

Kobayashi, N., & Nishida, K. (1998). Continuous excitation of planetary free oscillations by atmospheric disturbances. *Nature*, *395*(6700), 357–360. https://doi.org/10.1038/26427

Kurrle, D., & Widmer-Schnidrig, R. (2008). The horizontal hum of the Earth: A global background of spheroidal and toroidal modes. *Geophysical Research Letters*, *35*, L06304. https://doi.org/10.1029/2007GL033125

Lognonne, P., Clevede, E., & Kanamori, H. (1998). Computation of seismograms and atmospheric oscillations by normal-mode summation for a spherical Earth model with realistic atmosphere. *Geophysical Journal International*, *135*, 388–406.

Montagner, J.-P., Karczewski, J. F., Romanowicz, B., Bouaricha, S., Lognonné, P., Roult, G., … Koenig, J. C. (1994). The French pilot experiment OFM/SISMOBS: First scientific results on noise level and event detection. *Physics of the Earth and Planetary Interiors*, *84*(1–4), 321–336. https://doi.org/10.1016/0031-9201(94)90050-7

Nawa, K., Suda, N., Fukao, Y., Sato, T., Aoyama, Y., & Shibuya, K. (1998). Incessant excitation of the Earth's free oscillations. *Earth, Planets and Space*, *50*(1), 3–8. https://doi.org/10.1186/BF03352080

Nawa, K., Suda, N., Fukao, Y., Sato, T., Tamura, Y., Shibuya, K., … Kääriäinen, J. (2000). Incessant excitation of the Earth's free oscillations: Global comparison of superconducting gravimeter records. *Physics of the Earth and Planetary Interiors*, *120*(4), 289–297. https://doi.org/10.1016/S0031-9201(00)00158-8

Nishida, K. (2013). Earth's background free oscillations. *Annual Review of Earth and Planetary Sciences*, *41*(1), 719–740. https://doi.org/10.1146/annurev-Earth-050212-124020

Nishida, K., & Kobayashi, N. (1999). Statistical features of Earth's continuous free oscillations. *Journal of Geophysical Research*, *104*(28), 28,741–28,750. https://doi.org/10.1029/1999JB900286

Nishida, K., Kobayashi, N., & Fukao, Y. (2000). Resonant oscillations between the solid Earth and atmosphere. *Science*, *287*(5461), 2244–2246. https://doi.org/10.1126/science.287.5461.2244

Nishida, K., & Fukao, Y. (2007). Source distribution of Earth's background free oscillations. *Journal of Geophysical Research*, *112*, B06306. https://doi.org/10.1029/2006JB004720

Nishida, K., Montagner, J. P., & Kawakatsu, H. (2009). Global surface wave tomography using seismic hum. *Science*, *326*(112), 112.

Peterson, J. (1993). Observation and modeling of seismic background noise, U.S. Geol. Surv. Open File Report, 93-322: 1–95.

Rhie, J., & Romanowicz, B. (2004). Excitation of Earth's continuous free oscillations by atmosphere-ocean-seafloor coupling. *Nature*, *431*(7008), 552–556. https://doi.org/10.1038

Rhie, J., & Romanowicz, B. (2006). A study of the relation between ocean storms and the Earth's hum. *Geochemistry, Geophysics, Geosystems*, *7*, Q10004. https://doi.org/10.1029/2006GC001274

Romanowicz, B., Stakes, D., Montagner, J. P., Tarits, P., Uhrhammer, R., Begnaud, M., … Etchemendy, S. (1998). MOISE: A pilot experiment towards long-term sea-floor geophysical observatories. *Earth, Planets and Space*, *50*(11–12), 927–937. https://doi.org/10.1186/BF03352188

Stähler, S. C., Sigloch, K., Hosseini, K., Crawford, W. C., Barruol, G., Schmidt-Aursch, M. C., … Deen, M. (2016). Performance report of the RHUM-RUM ocean bottom seismometer network around la Réunion, western Indian Ocean. *Advances in Geosciences*, *41*, 43–63. https://doi.org/10.5194/adgeo-41-43-2016

Stephen, R. A., Spiess, F. N., Collins, J. A., Hildebrand, J. A., Orcutt, J. A., Peal, K. R., Ver- non, F. L., & Wooding, F. B. (2003). Ocean seismic network pilot experiment, *Geochemistry, Geophysics, Geosystems*, *4*(10), 1092. https://doi.org/10.1029/2002GC000485

Stutzmann, E., Montagner, J., Sebai, A., Crawford, W., Thirot, J., Tarits, P., … Etchemendy, S. (2001). Moise: A prototype multiparameter ocean-bottom station. *Bulletin of the Seismological Society of America*, *91*(4), 885–892. https://doi.org/10.1785/0120000035

Stutzmann, E., Roult, G., & Astiz, L. (2000). Geoscope station noise level. *Bulletin of the Seismological Society of America*, *90*, 690–701.

Suda, N., Nawa, K., & Fukao, Y. (1998). Earth's background free oscillations. *Science*, *279*(5359), 2089–2091. https://doi.org/10.1126/science.279.5359.2089

Sutherland, F. H., Vernon, F. L., Orcutt, J. A., Collins, J. A., & Stephen, R. A. (2004). Results from OSNPE: Low detection threshold magnitudes for ocean-bottom recording. *Bulletin of the Seismological Society of America*, *94*(5), 1868–1878. https://doi.org/10.1785/012003088

Taira, T., Zheng, Z., & Romanowicz, B. (2014). On the systematic long-period noise reduction on ocean floor broadband seismic sensors collocated with differential pressure gauges. *Bulletin of the Seismological Society of America*, *104*(1), 247–259. https://doi.org/10.1785/0120130015

Tanimoto, T. (2005). The oceanic excitation hypothesis for the continuous oscillations of the Earth. *Geophysical Journal International*, *160*(1), 276–288. https://doi.org/10.1111/j.1365-246X.2004.02484.x

Tanimoto, T., & Um, J. (1999). Cause of continuous oscillations of the Earth. *Journal of Geophysical Research*, *104*, 28,723–28,739. https://doi.org/10.1029/1999JB900252

Tanimoto, T. J. U., Nishida, K., & Kobayashi, N. (1998). Earths continuous oscillations observed on seismically quiet days. *Geophysical Research Letters*, *25*, 1553–1556.

Traer, J., & Gerstoft, P. (2014). A unified theory of microseisms and hum. *Journal of Geophysical Research: Solid Earth*, *119*, 3317–3339. https://doi.org/10.1002/2013JB010504

Watada, S., & Kanamori, H. (2010). Acoustic resonant oscillations between the atmosphere and the solid Earth during the 1991 Mt. Pinatubo eruption. *Journal of Geophysical Research*, *115*, B12319. https://doi.org/10.1029/2010JB007747

Webb, S. C. (2007). The Earth's 'hum' is driven by ocean waves over the continental shelves. *Nature*, *445*(7129), 754–756. https://doi.org/10.1038/nature05536

Webb, S. C., & Crawford, W. C. (1999). Long period seafloor seismology and deformation under ocean waves. *Bulletin of the Seismological Society of America*, *89*(6), 1535–1542.

Whittaker, J., Goncharov, A., Williams, S., Müller, D., & Leitchenkov, G. (2013). Global sediment thickness dataset updated for the Australian-Antarctic southern ocean. *Geochemistry, Geophysics, Geosystems*, *14*, 3297–3305. https://doi.org/10.1002/ggge.2018

Widmer, R., & Zürn, W. (1992). Bichromatic excitation of long-period Rayleigh and air waves by the mount Pinatubo and El Chichon volcanic eruptions. *Geophysical Research Letters*, *19*, 165–168. https://doi.org/10.1029/92GL00685

Widmer-Schnidrig, R. (2003). What can superconducting gravimeters contribute to normal-mode seismology? *Bulletin of the Seismological Society of America*, *93*, 1370–1380.

Zürn, W., & Widmer, R. (1995). On noise reduction in vertical seismic records below 2 mHz using local barometric pressure. *Geophysical Research Letters*, *22*, 3537–3540. https://doi.org/10.1029/95GL03369